

## On generating counter-rotating streamwise vortices

S H Winoto<sup>1</sup>, H Mitsudharmadi<sup>2</sup>, A C Budiman<sup>1</sup>, S M Hasheminejad<sup>1</sup>, T Nadesan<sup>1</sup>, Tandiono<sup>3</sup>, H T Low<sup>1</sup>, and T S Lee<sup>1</sup>

<sup>1\*</sup>formerly at National University of Singapore, Singapore 119260, now retired.

<sup>1</sup>National University of Singapore, Singapore 119260.

<sup>2</sup>formerly at Temasek Laboratory at National University of Singapore, Singapore 117411, now at Clean Combustion Research Center, KAUST, Thuwal 23955, Saudi Arabia.

<sup>3</sup>Institute of High Performance Computing, Singapore 138632.

E-mail: jacky.mucklow@iop.org

**Abstract.** Counter-rotating streamwise vortices are known to enhance the heat transfer rate from a surface and also to improve the aerodynamic performance of an aerofoil. In this paper, some methods to generate such counter-rotating vortices using different methods or physical conditions will be briefly considered and discussed.

### 1. Introduction

A well known method to enhance the heat transfer rate from a surface or to improve the aerodynamic performance of an aerofoil is by generating counter-rotating streamwise vortices in the surface or aerofoil boundary layer. Such method has recently attracted much interest due to the potential applications in fluid and thermal engineering. In this paper, some types of counter-rotating streamwise vortices which are generated using different methods or conditions will be briefly considered and discussed

### 2. Caused by centrifugal instability

The well known Görtler vortices which occur in concave surface boundary layer flows, as sketched in Fig.1, are in fact a system of counter-rotating streamwise vortices caused by centrifugal instability [1]. These vortices will appear if the Görtler number  $G_\theta$ , as defined by [2]:

$$G_\theta \geq (U_\infty \theta / R) \sqrt{\nu} \quad (1)$$

is greater than a critical value  $G_{\theta cr}$ , where  $\nu$  is the fluid kinematic viscosity,  $\theta$  the momentum thickness based on Blasius flat plate boundary-layer solution,  $U_\infty$  the free-stream velocity, and  $R$  the concave surface radius of curvature. The vortices will grow downstream resulting in a three-dimensional boundary-layer flow due to streamwise momentum distribution which causes spanwise variation in the boundary-layer thickness, due to the formation of the so-called “upwash” region, where low momentum fluid moves away from the surface, and the “downwash” region, where high speed outer fluid moves towards the surface (Fig. 1). At “upwash” regions, the boundary-layer is thicker and the shear stress is lower than those at “downwash” regions.

<sup>1</sup> To whom any correspondence should be addressed.



The effects of Görtler vortices on boundary layer development, heat transfer and deposition (for the case of turbine blades) cannot be ignored since concave surfaces exist in many fluid engineering applications.

Since the analytical work of Görtler [1], the early experimental works were mainly focused on visualizing these vortices to confirm their existence, as reviewed by Winoto *et al.* [3].

The heat transfer effect of Görtler vortices was first investigated by McCormack *et al.* [4] who reported 100 to 150% increase in Nusselt number on a concave surface in the presence of such vortices, compared with a reference flat plate. An empirical relationship for laminar heat transfer enhancement by the vortices was also proposed based on measurements on a turbine cascade [5]. The more recent works on the thermal effects of Görtler vortices were done by Crane & Sabzvari [6], Crane & Umur [7], and Momayez *et al.* [8, 9].

Numerical works on Görtler vortex instability were initially focused to find a unique stability curve. Floryan and Saric [10] found that the neutral curve appears to asymptotically level off at  $G_{0,cr} = 0.4638$  which can be considered as a critical value. Finnis & Brown [11] found that the minimum point of the unstable region occurs at  $G_0 = 1.38$  for the dimensionless wave number  $\alpha\theta = 0.28$ . Different values of  $G_{0,cr}$  were also obtained from experimental works. Moreover, Kottke & Mpourdis [12] did not detect any sign of instability when the screens that act as a source of disturbance were placed sufficiently far upstream. The above results show that the concept of a unique stability curve is not tenable in Görtler problem. The growth, as well as the wavelength selection mechanism of Görtler vortices, is fully governed by the receptivity process, as discussed by Denier *et al.* [13] and Bassom & Hall [14].

Assuming the most amplified vortices will occur in an experiment, a method based on the Görtler vortex stability diagram of Smith [2], for example, can be used to predict the experimental wavelength of Görtler vortices, for which the non-dimensional wavelength parameter  $\Lambda$  is defined as:

$$\Lambda = (U_\infty \lambda_m / \nu) (\lambda_m / R)^{0.5} \quad (2)$$

where  $\lambda_m$  is the most amplified Görtler vortex wavelength, and  $\Lambda$  represents a family of straight lines which cross the Görtler vortex stability diagram of  $G_0$  versus  $\alpha\theta$  where  $\alpha\theta$  is called dimensionless wave number and  $\alpha (= 2\pi/\lambda)$  is called wave number. Luchini & Bottaro [15] found that the most amplified wavelengths are for  $\Lambda = 220$  to  $270$ , while Floryan [16], Smith [2], and Meksyn [17] respectively proposed  $\Lambda = 210$ ,  $272$ , and  $227$ .

Since the wavelengths of naturally developed Görtler vortices are not uniform, experimental studies were biased due to the choice of “good” pairs of such vortices. Hence, Peerhossaini & Bahri [18], Ajakh *et al.* [19], Toe *et al.* [20] and Mitsudharmadi *et al.* [21, 22] used a series of thin wires placed upstream and perpendicular to the concave surface leading edge to pre-set or “force” the wavelength of Görtler vortices to be uniform and equal to the spanwise distance between the wires.

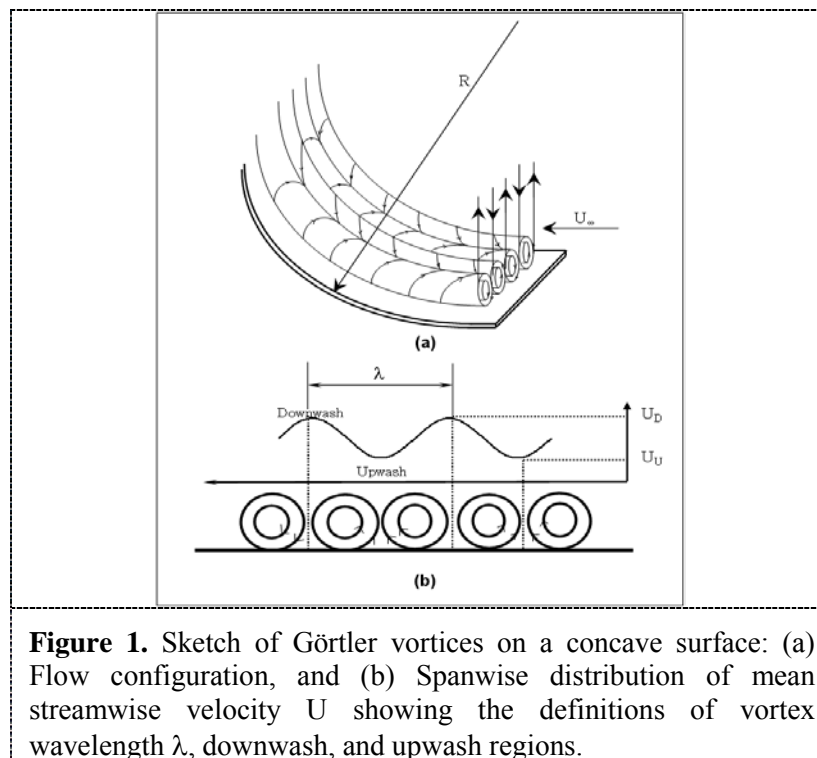


**Figure 1.** Sketch of Görtler vortices on a concave surface: (a) Flow configuration, and (b) Spanwise distribution of mean streamwise velocity  $U$  showing the definitions of vortex wavelength  $\lambda$ , downwash, and upwash regions.

Using hot-wire anemometer measurement, Mitsudharmadi *et al.* [23] were probably the first who experimentally showed the splitting and merging of Görtler vortices. The splitting of vortices occurred when the pre-set vortex wavelength was larger than the most amplified vortex wavelength  $\lambda_m$  and the merging occurred when the pre-set vortex wavelength was smaller than  $\lambda_m$ . Mitsudharmadi *et al.* [24] also experimentally confirmed the existence of its secondary instability.

Tandiono *et al.* [25] also used hot-wire anemometry to study the linear and non-linear development of Görtler vortices and later investigated the development of wall shear stress in concave surface boundary layer in the presence of Görtler vortices [26]. The wall shear stress  $\tau_w$  was “measured” or estimated by near-wall hot-wire measurements using the near-wall velocity gradient technique [27] on concave surface of 1.0 m radius of curvature in the presence of controlled Görtler vortices for three different. It was found that  $\tau_w$  at downwash decreases at a slightly lower rate than the Blasius curve, and increases after its minimum point. In contrast,  $\tau_w$  at upwash decreases at a higher rate than the Blasius curve. The minimum  $\tau_w$  is found to be 59% of the Blasius value at that position. After its minimum point,  $\tau_w$  increases slightly due to the secondary instability as the onset of secondary instability is just slightly before the location of the minimum  $\tau_w$  at the upwash [28]. The spanwise-averaged wall shear stress coefficient  $\bar{C}_f$ , which initially follows the Blasius curve, increases well above the local turbulent boundary layer value farther downstream due to the nonlinear effects of Görtler vortex instability and the secondary instability modes.

Görtler type vortices can also appear on flow over corrugated plates [29]. Flow in a channel with one of the simplest corrugation geometry of a sinusoidal plate is studied for which a corrugated plate with amplitude of 7.5 mm and wavelength of 78 mm, is mounted into a small wind tunnel. A flat plate is also mounted with the gap between these two plates is fixed at  $H = 50$  mm, as shown in Fig. 2. Layer of smoke is generated using smoke-wire flow visualization technique for which droplets of paraffin oil through the electrically heated thin wire and green laser sheet is mounted perpendicular to the channel. A digital camera is placed at certain distance after the exit of the wind tunnel to capture the visualization images.

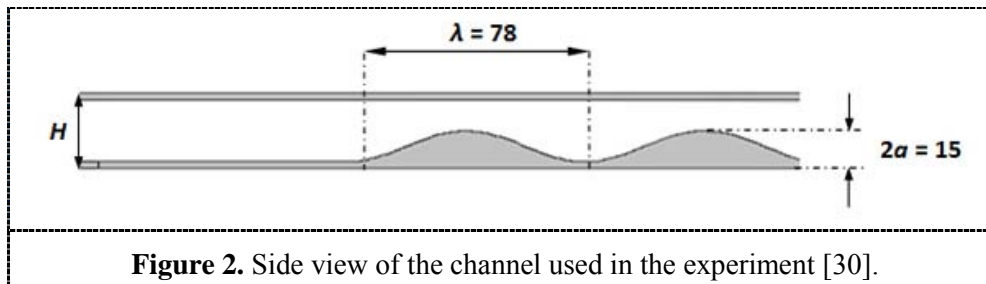


**Figure 2.** Side view of the channel used in the experiment [30].

From the smoke-wire flow visualization, the vortices can be found at the first peak of corrugation. In Fig. 3, for  $Re (= U_{\infty} \cdot \frac{1}{2}H / \nu) = 3350$ , at least two vortex structures are shown in the midspanwise plane. However, these naturally-developed vortex structures are not really similar since they have different spanwise wavelengths. Nevertheless, both structures show the stem and head of mushroom-like structures. The stem is related to the low momentum fluid that pulled out from the wall and returned back toward the wall with maximum shear and formed the mushroom hat [21]. Similar to the concave surface case, these two structures refer to the most amplified counter-rotating vortices.

Non-uniformity in size and in spanwise wavelength of such vortices will cause experimental bias in studying the phenomenon [31]. Thus, to obtain a more uniform size and wavelength for such vortices, for example as shown in Fig. 4, it is necessary to pre-set the vortex wavelength by some geometric patterns like triangles on the flat plate leading edge. This patterned leading edge is used as a substitute for perturbation wires used in some earlier works, such as by Peerhossaini & Bahri [18] and Ajakh *et al.* [19].

From the visualization, the downstream development of the vortices is also examined. After the first peak, separation bubble formed at the valley of corrugation and the vortices were floating above it. These vortices remained visible until the second valley, where the mixing of the flow was improved and the structures broke down prior to turbulence. As the Reynolds number increased, the onset of turbulence is moved upstream. While for  $Re = 3350$  the vortices remain visible up to the second peak, for  $Re = 5300$  the vortex structures can be clearly observed only at the first peak.

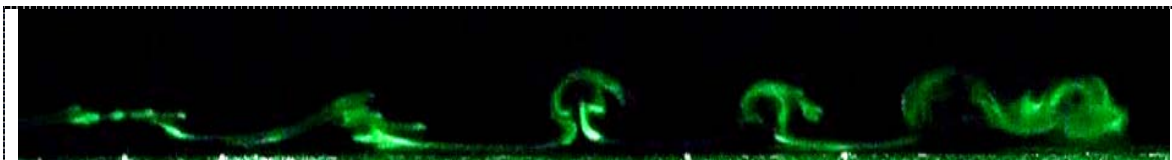


**Figure 3.** Two naturally-developed counter-rotating Görtler type vortices in the middle of the spanwise plane at the first peak of corrugation, caused by the centrifugal effect from sinusoidal plate. In this case,  $Re = 3350$ .



**Figure 4.** Counter-rotating Görtler type vortices with nearly uniform spanwise wavelength at the first peak of sinusoidal plate with the modified leading edge,  $Re = 3350$  (taken from [30]).

### 3. Caused by leading edge patterns

Some simple geometric patterns on the leading edge of a flat plate or an airfoil, patterns, such as, saw tooth shape, can generate counter-rotating streamwise vortices in the surface boundary layer flow which can improve momentum exchange which results in a better mixing zone and increased heat transfer.

The use of leading edge pattern was actually inspired by nature, for example, the owl wings generate mini vortices by comb like feathers, so to retard the boundary layer separation, and consequently, give this predator the ability of quietly approaching its prey by high stall angle of attack [32]. These vortices were interpreted like vortex lift over the delta wings, which create low pressure region over the surface. As the angle of attack increases, the vortex lift increases until it breaks down.

Studies by Fish and Battle [33] on humpback whales' pectoral flipper demonstrated that the flipper has high aspect ratio, symmetric profile with large sinusoidal tubercles (protuberances on the leading edge) which can cause a considerable increase in the stall angle of attack and the maximum lift coefficient. The combination of tubercles and the high aspect ratio of the flippers allow humpback whale to perform sharp banking turns lead to a rise in proportion of lift to drag coefficients [34] despite of its huge and inflexible body.

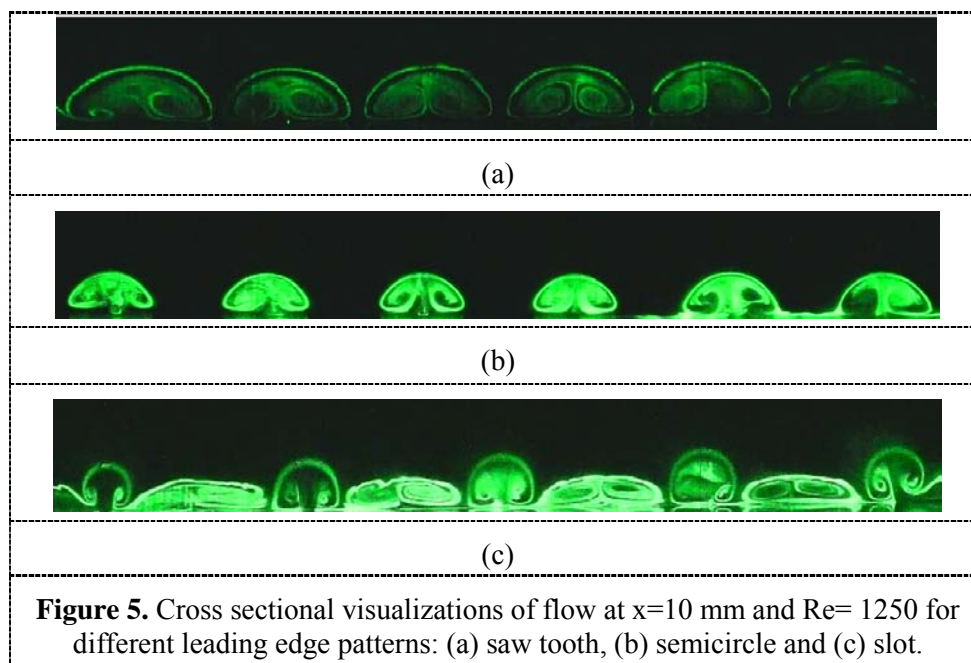
These examples help to better understand the actual mechanism of the leading edge shape on generating vortices. Soderman [35] examined the effect of attached saw-tooth to the leading edge of a 2-D airfoil and found that this type of leading edge can reduce the separation and drag. Johari *et al.* [36] experimentally studied the role of sinusoidal protuberances on the leading edge of a 2-D airfoil. They determined that the amplitude of the protuberances plays more significant role on the performance than the wavelength and also found from visualization that the flow separation forms chiefly in the region between two ridges. Cranston *et al.* [37] recently showed the size of the serrations on flat plates at low Reynolds numbers significantly affects the aerodynamic characteristics and separation bubble.

Some practical applications have been considered, for example, Weber *et al.* [38] used tubercles on the leading edge of rudder and found the tubercles enhance lift for high angles of attack. It causes more favourable control during turning.

An industrial fan with leading edge protuberances on blades was reported to produce higher flow rates at lower speeds and lower noise level and hence improved its efficiency and electricity consumption [39]. The use of tubercles technology has also been successfully applied in renewable power generation. A 35 kW wind turbine utilizing tubercles technology on its blades was recently introduced. This new design produced more electricity at more moderate wind speeds [40].

Since the mechanism of the leading edge pattern on the flow structures and the effective parameters are still not well understood yet, Hasheminejad *et al.* [41] studied the effect of different leading edge patterns on the vortex structures generated using smoke visualizations on a flat plate with 14 mm wavelength of saw-teeth, semi-circulars and slots. The experiments were performed in a small open-circuit low speed wind tunnel with its test section of 160mm x 160mm and free-stream turbulent intensity of about 0.25%. The smoke-wire flow visualization was used to visualize the cross-sections of the vortex structures generated in the flat plate boundary layers at some streamwise positions from the flat plate leading edge for different Reynolds numbers (based on wavelength of leading edge patterns) ranging from 1250 to 1800.

For all the leading edge patterns considered, the visualization results show that pairs of counter-rotating vortices are formed in the laminar part of boundary layer and grow in the streamwise direction until they break down to turbulence. However, for the case of the leading edge with slots, there are additional counter-rotating vortices which occur in the spaces between the slots which may be a secondary flow caused by the intense upwash flow made by the abrupt change of the flow direction in a narrow span. The cross-sections of the vortex structures due to different leading edge patterns are visualized in Fig. 5. Hot-wire anemometer measurements within these vortex structures will be conducted to obtain quantitative data.



#### 4. Due to vortex generator

Mushroom like counter-rotating vortex pairs are predominant structures that occur in the transitional boundary layers [42]. To study the dynamics of these vortices in the transitional boundary layer, evolving spatially and temporally, is cumbersome [43]. Hence, a more convenient environment to characterize these embedded vortices is necessary. Görtler vortex system is a good example to characterize such vortices since they appear as steady, spatially evolving structures in concave surface laminar boundary layer flow. Initiation or simulation of such counter-rotating streamwise vortex pair in a zero pressure gradient flat plate boundary layer is possible by passive means, such as vortex generators which have been effectively employed in aerodynamics for flow control, as well as in heat transfer enhancement. There are many different types of vortex generators and a brief overview is given by Lin [44].

Besides the vortex generators, scales of fast swimming sharks were reported to have directional surface roughness elements known as convergent and divergent riblets [45,46]. Recently, the application of convergent and divergent riblets in manipulating turbulent boundary layer, to reduce the skin friction drag and to control very large scale motion, was initiated [47]. The highly inflexional velocity profiles created around the center of convergence, by these roughness elements are similar to those of Görtler vortices [45,48]. The convergent and divergent riblets used in these studies consist of multiple riblets arranged in tandem with a constant pitch. The aim of this work is to incorporate a single set of convergent riblets (Fig. 6) in a flat plate boundary layer to study the growth and formation of these vortices using smoke-wire visualization technique.

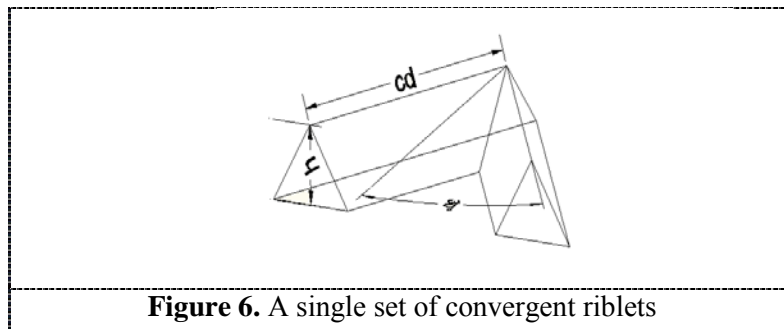


**Figure 6.** A single set of convergent riblets

The experiment was carried out on a flat plate where a single set of convergent riblets are mounted. The riblet height is 1mm and the aspect ratio of the riblet is defined as the ratio of  $cd$  to  $h$ , which is set to 2 in this study, where  $cd$  is the riblet length. The riblet set is placed at a distance from the leading edge such that the ratio of Blasius boundary layer thickness to the height of the riblet ( $\delta/h$ ) is 0.5. The angle of the riblet to the flow is  $30^\circ$  as shown in Fig. 6. The model is mounted inside a low speed wind tunnel with free stream turbulent intensity of about 0.25% and with test section of 160 x 160mm cross-section. Smoke sheet is created by applying a constant current through a wire coated by paraffin oil dripped along through gravity. The co-ordinates has its origin at the trailing end of the riblets. Any distance mentioned henceforth is with respect to the origin.

As shown in Fig. 7, the vortices are initiated by the convergent riblets grows along the downstream direction. The mushroom like structure comprises the stem and the counter-rotating vortex pair distributed on its either side. As the flow encounters the convergence, the fluid stream in the boundary layer, encountering the riblets, is lifted up due to continuity thus initiating a transverse velocity. The low momentum fluid from the boundary layer is lifted up to a distance until it overcomes the normal pressure gradient. As the low momentum fluid is ejected away from the wall, the outer high momentum fluid tries to penetrate the boundary layer to satisfy continuity. The high momentum fluid thus envelopes to form the mushroom hat exhibiting maximum shear stress, similar to Görtler vortices.

Along the downstream direction, the vortices gets tilted which might indicate the onset of transition as shown in Fig. 7 (c) and far downstream, the structures broke down. As the ratio  $\delta/h$  decreased, the observed phenomenon occurred earlier upstream.

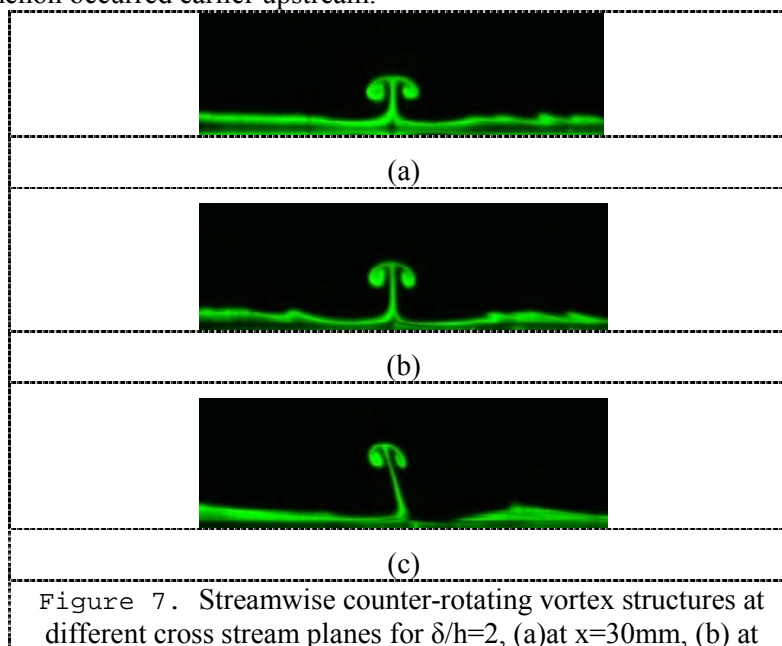


**Figure 7.** Streamwise counter-rotating vortex structures at different cross stream planes for  $\delta/h=2$ , (a) at  $x=30\text{mm}$ , (b) at

x=60mm, and (c) at x=150mm.

## 5. Conclusions

Some types of counter-rotating streamwise vortices generated by different methods or physical conditions have been briefly considered and visualized using smoke-wire flow visualization technique. The experimental work on these vortices are still on going to obtain quantitative data from the vortex structures by means of hot-wire anemometry and/or particle image velocimetry.

## 6. Acknowledgement

The authors would like to thank the Temasek Laboratories at the National University of Singapore (NUS) for conducting some of the experiments at its Aeroscience Laboratory.

The third, fourth and fifth authors are currently recipients of the NUS Research Scholarship, while the second and sixth authors are former recipients of the NUS Research Scholarship.

## 7. References

- [1] Görtler, H., Über eine dreidimensionale Instabilität laminarer Grenzschichten an konkaven Wänden, *Ges. D. Wiss. Göttingen, Nachr. a. d., Math.*, 2 (1) (1940); translated as "On the three-dimensional instability of laminar boundary layers on concave walls", NACA TM 1375, 1954.
- [2] Smith, A.M.O., On the growth of Taylor-Görtler vortices along highly concave wall, *Quart. Appl. Mech.*, 13, pp 233-262, 1955.
- [3] Winoto, S.H., Mitsudharmadi, H. and Shah, D.A., Visualizing Görtler vortices, *Journal of Visualization*, 8, no. 4, pp 315-322, 2005.
- [4] McCormack, P.D., Welker, H. and Kelleher, M., Taylor- Görtler vortices and their effect on heat transfer, *ASME Journal of Heat Transfer*, 92, pp. 101-112, 1970.
- [5] Kan, S., Miwa, K., Morishita, T., Munakata, Y. and Nomura, M., Heat transfer of a turbine blade, *Proceedings of Joint International Gas Turbine Conference*, Tokyo, Japan, October 4-7, pp 219-226, 1971.
- [6] Crane, R.I. and Sabzvari, J., Heat transfer visualization and measurement in unstable concave-wall boundary layers, *ASME Journal of Turbomachinery*, 111, pp 51-56, 1989.
- [7] Crane, R.I. and Umur, H., Concave-wall laminar heat transfer and Görtler vortex structure: Effects of pre-curvature boundary layer and favourable pressure gradients, *ASME Paper No. 90-GT-94*, 1990.
- [8] Momayez, L., Dupont, P. and Peerhossaini, H., Some unexpected effects of wavelength and perturbation strength on heat transfer enhancement by Görtler instability, *International Journal of Heat and Mass Transfer*, 47, pp 3783-3795, 2004a.
- [9] Momayez, L., Dupont, P. and Peerhossaini, H., Effects of vortex organization on heat transfer enhancement by Görtler instability, *International Journal of Thermal Sciences*, 43, pp 753-760, 2004b.
- [10] Floryan, J.M. and Saric, W.S., Stability of Gortler vortices in boundary layers, *AIAA Journal*, 20, no. 3, pp 316-324, 1982.
- [11] Finnis, M.V. and Brown, A., Stability of a laminar boundary-layer flowing along a concave surface, *ASME Journal of Turbomachinery*, 111, pp 376-386, 1989.
- [12] Kottke, V and Mpouradis, B, On the existence of Taylor-Görtler vortices on concave walls, *Proceedings of the 4<sup>th</sup> International Symposium on Flow Visualization*, Paris, 1986, pp. 475-480, Hemisphere Publishing Corp., Washington, 1987.
- [13] Denier, J.P., Hall, P., and Seddougui, S.O., On the receptivity problem for Görtler vortices: vortex motions induced by wall roughness, *Philosophical Transactions: Physical Sciences and Engineering*, 335, no. 1636, pp 51-85, 1991
- [14] Bassom, A.P. and Hall, P., The receptivity problem for O(1) wavelength Görtler vortices, *Proceedings of Mathematical and Physical Sciences*, 446, no. 1928, pp 499-516, 1994

- [15] Luchini, P. and Bottaro, A, Görtler vortices: a backward-in-time approach to the receptivity problem, *Journal of Fluid Mechanics*, 363, pp 1-23, 1998
- [16] Floryan, J.M., On the Görtler instability of boundary-layer, *Progress in Aerospace Science*, 28, pp 235-271, 1991.
- [17] Meksyn, D., Stability of viscous flow over concave cylindrical surfaces, *Proceedings .Roy. Soc.*, 203, no. 1073, pp 253-265, 1950.
- [18] Peerhossaini, H. and Bahri, F., On the spectral distribution of the modes in non-linear Görtler instability, *Experimental Thermal and Fluid Science*, 16, no. 3, pp 195-208, 1998.
- [19] Ajakh, A., Kestoras, M.D., Toe, R., and Peerhossaini, H., Influence of Forced Perturbation in the Stagnation Region on Görtler Instability, *AIAA Journal*, 37, no. 12, pp 1572-1577, 1999.
- [20] Toe, R., Ajakh, A., and Peerhossaini, H., Heat transfer enhancement by Görtler instability, *International Journal of Heat and Fluid Flow*, 23, no. 2, pp 194-204, 2002.
- [21] Mitsudharmadi, H., Winoto, S. H. and Shah, D. A., Development of boundary layer flow in the presence of forced wavelength Görtler vortices, *Physics of Fluids*, Vol. 16, no. 11, pp 3983-3996, 2004.
- [22] Mitsudharmadi, H., Winoto, S.H. and Shah, D.A., Development of most amplified wavelength Görtler vortices, *Physics of Fluids*, no. 18, 014101, 1 – 12, 2006.
- [23] Mitsudharmadi, H., Winoto, S.H., and Shah, D.A., Splitting and merging of Görtler vortices, *Physics of Fluids*, no. 17, 124102, 1 – 12, 2005.
- [24] Mitsudharmadi, H., Winoto, S.H., and Shah, D.A., Secondary instability in forced wavelength Görtler vortices, *Physics of Fluids*, no. 17, 074104, 1 – 8, 2005.
- [25] Tandiono, Winoto, S.H. and Shah, D.A., On the linear and nonlinear development of Görtler vortices, *Physics of Fluids*, 20, no. 8, 094103, 1 – 15, 2008.
- [26] Tandiono, Winoto, S.H. and Shah, D.A., Wall shear stress in Görtler vortex boundary layer flow, *Physics of Fluids*, 21, no. 8, 084106, 1 – 9, 2009.
- [27] Hutchins, N. & Choi, K.S., Accurate measurements of local skin friction coefficient using hot-wire anemometry, *Progress in Aerospace Sciences* 38 (4-5), 421, 2002.
- [28] Bottaro, A. & Klingmann, B. G. B., On the linear breakdown of Görtler vortices, *European Journal of Mechanics, B/Fluids*, 15 (3), 301, 1996
- [29] Nishimura, T., Yano, K., Yoshino, T., & Kawamura, Y. 1990. Occurrence and structure of Taylor-Goertler vortices induced in two-dimensional wavy channels for steady flow. *Journal of Chemical Engineering of Japan*, no. 23 (6), pp. 697-703
- [30] Budiman, A.C., Mitsudharmadi, H., Low, H.T. & Winoto, S.H. Visualization of counter-rotating streamwise vortices in a rectangular channel with one-sided wavy surface. *Proceeding of the 31<sup>st</sup> AIAA Applied Aerodynamics Conference*. San Diego, CA., 2013.
- [31] Mitsudharmadi, H., Jamaludin, M.N.A. & Winoto, S.H. Streamwise vortices in channel flow with a corrugated surface. *Proceedings of the 10th WSEAS International Conference on Fluid Mechanics & Aerodynamics (FMA'12)*. Istanbul, Turkey, 2012.
- [32] Anderson, G., W. An Experimental Investigation of a High-Lift Device on the Owl Wing. Master Dissertation, Air Force Institute of Technology, Wright-Patterson Air Force Base, Ohio, 1973
- [33] Fish, F.E & Battle, J. M. Hydrodynamic Design of the Humpback Whale Flipper. *Journal of Morphology*, 225, pp. 51-60, 1995.
- [34] Fish, F.E., Weber, P.W., Murray, M., M. & Howle, E.. The Tubercles on Humpback Whales' Flipper: Application of Bio- Inspired Technology, Vol. 51, number 1, pp 203-213, 2011.
- [35] Soderman, P, T. Aerodynamic Effects of Leading Edge Serrations on a Two-Dimensional Airfoil. National Aeronautics and Space Administration. Ames Research Center, Moffett Field, CA, 1972.
- [36] Johari, H., Henoeh, C., Custodio, D., and Levshin, A. 2007. Effects of Leading-Edge Protuberances on Airfoil Performance. *AIAA Journal*, Vol. 45, No. 11, Nov. pp 2634–2642.

- [37] Cranston, B., Laux, C., Altman, A. 2012. Leading Edge Serrations on Flat Plates at Low Reynolds Number. 50th AIAA Aerospace Sciences Meeting including the New Horizons Forum and Aerospace Exposition, Nashville, Tennessee, 0053.
- [38] Weber, P., W., Howle, L., E., Murray, M., M. 2010. Lift, drag and cavitation onset on rudders with leading edge tubercles. *Mar Tech* 47:27–36.
- [39] Ontario Power Authority. 2010. Energy efficient fans take their cue from the humpback whale. [http://archive.powerauthority.on.ca/Storage/122/16957\\_AgNews\\_July231.pdf](http://archive.powerauthority.on.ca/Storage/122/16957_AgNews_July231.pdf).
- [40] Howle, L.E. WhalePower Wenvor blade. A report in the efficiency of a WhalePower Corp. 5 meter prototype wind turbine blade. BelleQuant Engineering, PLLC, 2009.
- [41] Hasheminejad, S., M., Mitsudharmadi, H. & Winoto S., H. Visualization of Boundary Layer on Flat Plate with Leading Edge Patterns. 2013. 12<sup>th</sup> Asian Symposium on Visualization, Tainan, Taiwan.
- [42] Bernard, P.S. The hairpin vortex illusion. *Journal of Physics*. 318, 2011.
- [43] Swearingen J.D. & Blackwelder R.F., The growth and breakdown of streamwise vortices in the presence of a wall. *Journal of Fluid Mechanics*. Vol.182, pp. 255-290, 1987
- [44] Lin J.C., Review of low profile vortex generators to control boundary layer separation, “Progress in Aerospace Sciences. 38, pp.389-420, 2002.
- [45] Koeltzsch, K, Dinkelacker, A & Grundmann, R. Flow over convergent and divergent wall riblets, *Experiments in Fluids*. Vol. 33, pp. 346 - 350, 2002.
- [46] Nugroho, B, Kulindaivelu, V, Harun, Z, Hutchins, N & Monty, J. P. An investigation into the effects of highly directional surface roughness on turbulent boundary layers, *Proceedings of the 17<sup>th</sup> Australasian Fluid Mechanics Conference*, Auckland, New Zealand, 2010.
- [47] Nugroho, B, Hutchins, N, & Monty, J. P. Effects of diverging and converging roughness on turbulent boundary layers. *Proceedings of the 18<sup>th</sup> Australasian Fluid Mechanics Conference*, Launceton, Australia, 2012.
- [48] Nadesan, T, Mitsudharmadi, H, Lee, T.S. & Winoto, S.H.. Effects of converging riblets in flat plate boundary layer, *The 12<sup>th</sup> International Symposium of Fluid Control Measurement and Visualization*, Nara, Japan, 2013.